ELSEVIER

Thermochimica Acta 275 (1996) 269–278

thermochimica acta

Preparation and thermal decomposition of solid state compounds of 4-methoxybenzylidenepyruvate with alkali earth metals, except beryllium and radium

L.C.S. de Oliveira [a], D.E. Rasera [a], O.S. Siqueira [b], J.R. Matos [c], C.B. Melios [a], M. Ionashiro [a,*]

[a] *Instituto de Química, Universidade Estadual Paulista, Araraquara, S.P., C.P. 355, CEP. 14800-900, Brazil*

[b] *Dept° de Química, Universidade Federal do Mato Grosso do Sul, Campo Grande, M.S., C.P. 649, CEP. 79070-900, Brazil*

[c] *Instituto de Química, Universidade de São Paulo, São Paulo, S.P., C.P. 20780, CEP. 01498-970, Brazil*

Received 3 October 1994; accepted 7 May 1995

Abstract

Solid compounds of general formula $ML_2 \cdot nH_2O$ [where M is Mg, Ca, Sr or Ba; L = 4 methoxybenzylidenepyruvate (4-MeO-BP); $n = 4$, 1 or 0] have been synthetized. Thermogravimetry (TG), derivative thermogravimetry (DTG), differential scanning calorimetry (DSC), x-ray diffraction powder patterns and elemental analysis have been used to characterize the compounds. The thermal stability of these compounds as well as that of the decomposition products were studied using Pt or Al_2O_3 crucibles in an air or a CO_2 atmosphere.

Keywords: 4-Methoxybenzylidenepyruvate; Alkali earth metals; Thermal decomposition

1. Introduction

Several metal ion complexes with 4-methoxybenzylidenepyruvate (CH_3–O–CH=CH–$COCOO^-$, abbreviated as 4-MeO-BP) have been studied in aqueous solution [1–3]. The synthesis and thermal stability of solid compounds of 4-MeO-BP with trivalent lanthanides and yttrium have also been reported [4].

* Corresponding author.

SSDI 0040-6031(95)02536-7

The present paper is an extension of previous research [4]. We report here the synthesis and thermal stability of solid compounds of general formula $ML_2 \cdot nH_2O$ (where M = Mg, Ca, Sr or Ba, L is 4-MeO-BP and $n = 4$, 1 or 0). They were characterized by elemental analysis, TG and DTG analysis, DSC studies and X-ray diffraction powder patterns.

2. Experimental

The sodium salt of 4-MeO-BP was prepared as described in the literature [5]. Aqueous solutions of the metal (Mg, Ca, Sr or Ba) were prepared by dissolving the respective metal chlorides. The metal ion compositions of these solutions were determined by complexometric titrations with standard EDTA solutions [6]. The solid compounds of the alkali earth metals with 4-MeO-BP were prepared from the aqueous solutions of the metal ions and the aqueous solution of Na(4-MeO-BP), as previously described [4]. The metal contents of the compounds were determined by complexometric titrations with standard EDTA solution [6], after samples of the compounds had been ignited to the metal oxide or carbonate and dissolved in water. Metal contents were also determined from the TG curves. The water and 4-MeO-BP contents were determined from the TG curves and confirmed by carbon and hydrogen microanalytical determinations.

The TG, DTG and DSC curves were obtained using a Mettler TA-4000 thermoanalyser system with air or CO_2 flowing at a rate of about 150 ml min^{-1}, and a heating rate of 10°C min^{-1}, with samples weighing about 7 mg. Alumina or platinum crucibles with perforated covers were used to obtain the TG and DTG curves. Aluminium crucibles with perforated covers were used to obtain the DSC curves.

X-ray powder patterns were obtained with an HGZ 4/B horizontal diffractometer (GDR) equipped with a proportional counter and pulse height discriminator. The Bragg-Brentano arrangement was adopted using CuKα radiation ($\lambda = 1.541$ Å) and a setting of 38 kV and 20 mA.

Carbon and hydrogen were determined by microanalytical procedures using a Perkin-Elmer Elemental Analyser.

3. Results and discussion

Table 1 presents the analytical and thermoanalytical data of the compounds of general formula $M(4\text{-MeO-BP})_2 \cdot nH_2O$.

The X-ray diffraction powder patterns (Fig. 1) show that the strontium and barium compounds are isomorphous. All the compounds have crystalline structures.

The TG and DTG curves of the compounds are shown in Fig. 2 in the sequence: air–Pt, air–Al_2O_3, CO_2–Pt, and CO_2–Al_2O_3. All the compounds lose mass in several steps. The patterns of the TG and DTG curves are characteristic for each compound. The curves also show the influence of the crucibles and of the atmospheres used during the thermal decomposition of these compounds. The anhydrous compound produced

Table 1
Analytical data of the compounds $M(L)_2 \cdot nH_2O$

	M(%)			L(%)		Water(%)		C(%)		H(%)	
Compound	Calcd.	EDTA	TG	Calcd.	TG	Calcd.	TG	Calcd.	E.A.	Calcd.	E.A.
$MgL_2 \cdot 4H_2O$	4.79	4.72	4.80	77.82	78.24	14.23	14.16	52.14	52.19	5.17	5.11
$CaL_2 \cdot H_2O$	8.55	8.58	8.84	84.18	83.53	3.85	4.11	56.40	56.25	4.30	4.32
$SrL_2 \cdot H_2O$	16.98	16.60	17.11	67.90	67.94	3.49	3.40	51.42	51.67	3.92	3.89
BaL_2	25.07	24.49	25.35	63.97	57.37[a]	–	–	48.24	48.11	3.31	3.31

Key: M, alkali earth metal; L, 4-methoxybenzylidenepyruvate.
[a] Final thermal decomposition > 900°C.

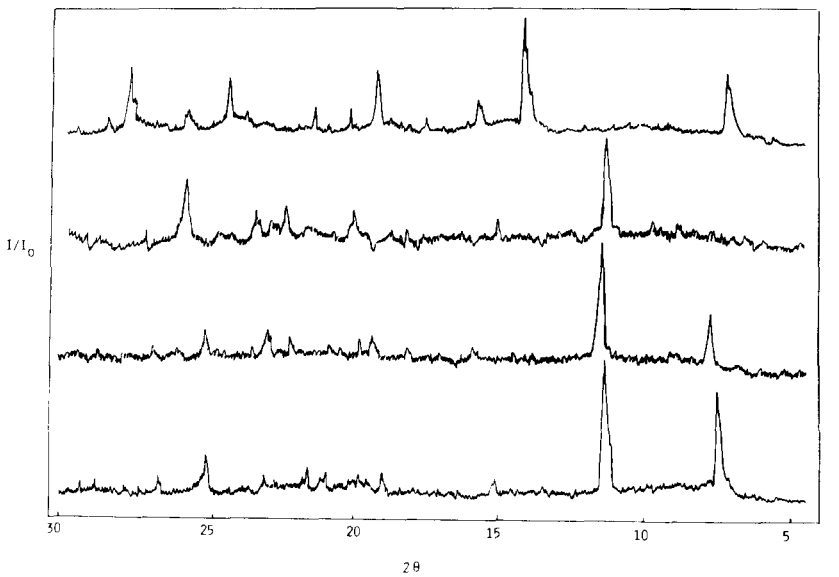

Fig. 1. X-ray powder diffraction patterns of $Mg(4\text{-MeO-BP})_2.4H_2O$, $Ca(4\text{-MeO-BP})_2.H_2O$, $Sr(4\text{-MeO-BP})_2.H_2O$ and $Ba(4\text{-MeO-BP})_2$.

in a CO_2 atmosphere was more stable than that produced in air. For the same atmosphere, the final thermal decomposition temperature in an alumina crucible was higher than that in a platinum crucible. A great similarily in the curves was also observed for the same atmosphere in both kinds of crucibles.

For the compound of magnesium, the TG and DTG curves (Figs. 2(a)–(d)) show that the dehydration occurs in two consecutive steps and that the resulting anhydrous compound decomposes in a process comprising several steps of mass loss. The curves are similar (except for air–Pt), suggesting that the decomposition mechanism is the same. For all the curves, MgO is observed as a residue of the decomposition. The exception is in the CO_2–Al_2O_3 conditions where the mass loss continues up to 900°C.

Under several conditions, the TG and DTG curves for the calcium and strontium compounds (Fig. 2(e)–(l)) show a first mass loss due to dehydration. The thermal decomposition of the resulting anhydrous compounds is similar in air and CO_2 atmosphere, and the temperatures at which the partial thermal decompositions occur are lower for platinum than for alumina crucible. For the calcium compound, the final residue in air atmosphere is calcium oxide; while in CO_2 the final residue is calcium carbonate for both crucibles. For the strontium compound, the final residue is strontium carbonate in either atmosphere or crucible.

For the barium compound, the TG and DTG curves (Figs. 2(m)–(p)) show mass losses in several consecutive steps and a great similarity is observed in all the curves

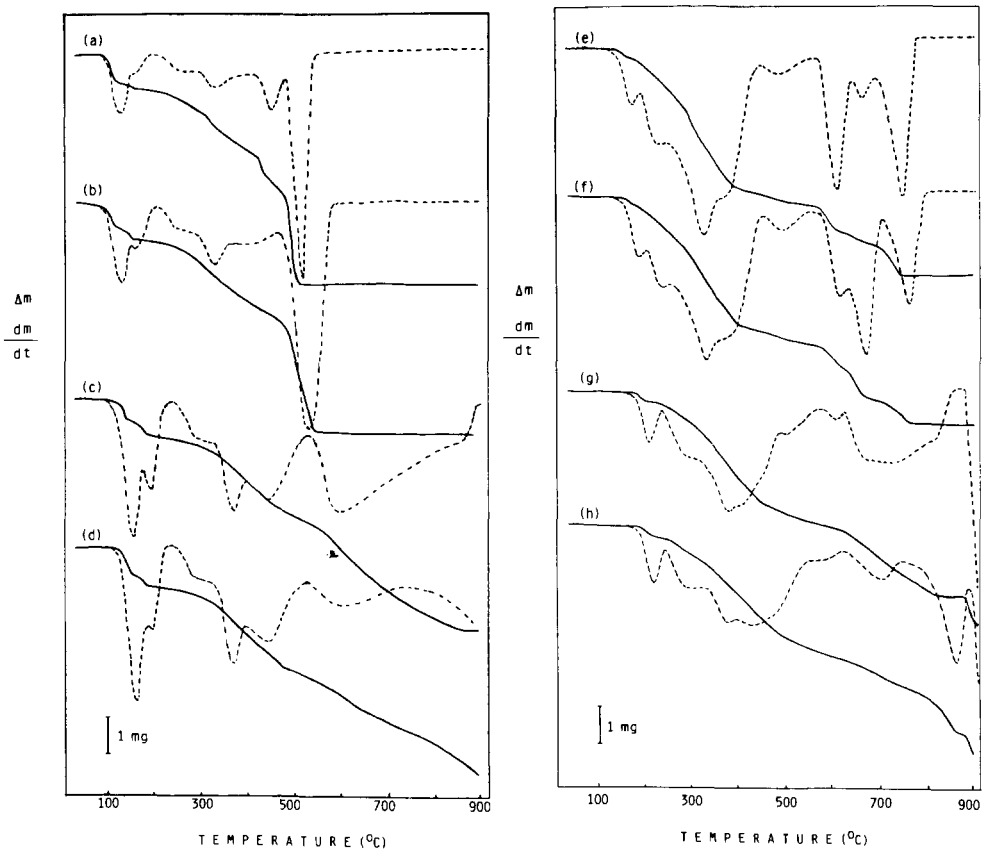

Fig. 2. TG-DTG curves of the compounds: (a) $Mg(4\text{-}MeO\text{-}BP)_2.4H_2O$ (Pt–air, 7.004 mg); (b) $Mg(4\text{-}MeO\text{-}BP)_2.4H_2O$ (Al_2O_3–air, 7.050 mg); (c) $Mg(4\text{-}MeO\text{-}BP)_2.4H_2O$ (Pt–CO_2, 7.166 mg); (d) $Mg(4\text{-}MeO\text{-}BP)_2.4H_2O$ (Al_2O_3–CO_2, 7.176 mg); (e) $Ca(4\text{-}MeO\text{-}BP)_2.H_2O$ (Pt–air, 7.001 mg); (f) $Ca(4\text{-}MeO\text{-}BP)_2.H_2O$ (Al_2O_3–air, 7.178 mg); (g) $Ca(4\text{-}MeO\text{-}BP)_2.H_2O$ (Pt–CO_2, 7.135 mg); (h) $Ca(4\text{-}MeO\text{-}BP)_2.H_2O$ (Al_2O_3–CO_2, 7.135 mg); (i) $Sr(4\text{-}MeO\text{-}BP)_2.H_2O$ (Pt–air, 7.052 mg); (j) $Sr(4\text{-}MeO\text{-}BP)_2.H_2O$ (Al_2O_3–air, 7.135 mg); (k) $Sr(4\text{-}MeO\text{-}BP)_2.H_2O$ (Pt–CO_2, 7.140 mg); (l) $Sr(4\text{-}MeO\text{-}BP)_2.H_2O$ (Al_2O_3–CO_2, 7.075 mg); (m) $Ba(4\text{-}MeO\text{-}BP)_2$ (Pt–air, 7.070 mg); (n) $Ba(4\text{-}MeO\text{-}BP)_2$ (Al_2O_3–air, 7.076 mg); (o) $Ba(4\text{-}MeO\text{-}BP)_2$ (Pt–CO_2, 7.136 mg) and (p) $Ba(4\text{-}MeO\text{-}BP)_2$ (Al_2O_3–CO_2, 6.991 mg).

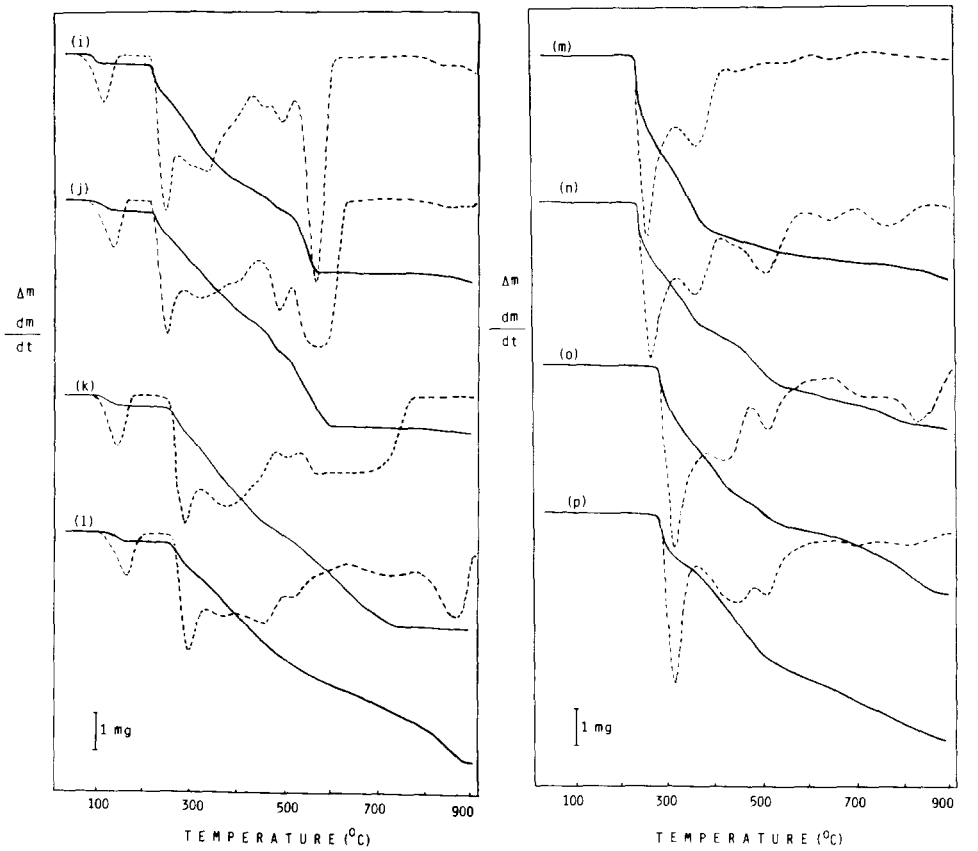

Fig. 2. *(Continued)*

obtained in both atmospheres. Although the DTG curves show mass losses in several steps, the TG curves suggest two consecutive mass losses with the same thermal decomposition mechanism, except for the air–Al_2O_3 conditions where the TG curve shows three consecutive steps. These curves also show that the mass losses are still being observed up to 900°C with formation of barium carbonate and carbonaceous residue, even in an air atmosphere.

In the TG and DTG curves where the formation of carbonate as a residue was observed, tests with hydrochloric acid on samples heated until the temperature indicated by the TG and DTG curves confirmed the presence of carbonate anion, or carbonate anion together with a carbon residue.

The mass losses and the corresponding temperature ranges for the partial thermal decomposition of all the compounds are shown in Table 2.

The DSC curves of the compounds in air or CO_2 atmosphere are shown in Fig. 3. These curves show endothermic and exothermic peaks that are all in accord with the mass losses of the TG and DTG curves up to 600°C, and peaks attributed to recrystallization processes or crystalline transitions.

Table 2
Thermoanalytical data of the compounds $M(L)_2nH_2O$

Compound m_i/mg condition	Mass loss/ (mg)	Temp. range/°C	Attribution	Mass loss%	
				Obs.	Calcd.
$MgL_2 \cdot 4H_2O$	0.744	84–122	$3H_2O$	10.62	10.67
7.004	0.248	122–162	$1H_2O$	3.54	3.56
Air–Pt	0.866	204–316	2(CH–O–)	12.36	12.25
	1.084	316–424		15.48	15.02
	1.049	424–486		14.98	15.02
	2.481	486–515	Residue of the ligand	35.42	35.54
7.050	0.615	82–120	2.5HO	8.72	8.89
Air–Al_2O_3	0.340	120–168	1.5HO	5.65	5.34
	0.870	204–314	2(CH–O–)	12.34	12.25
	1.095	314–430		15.53	15.02
	3.520	430–550	Residue of the ligand	49.94	50.56
7.166	0.527	100–150	$2H_2O$	7.35	7.11
CO_2–Pt	0.514	150–194	$2H_2O$	7.17	7.11
	0.867	244–364	2(CH–O–)	12.09	12.25
	1.079	364–460		15.06	15.02
	3.589	460–870	Residue of the ligand	50.08	50.56
7.176	0.661	112–152	$2.5H_2O$	9.21	8.89
CO_2–Al_2O_3	0.349	152–194	$1.5H_2O$	4.86	5.34
	0.855	244–364	2(CH–O–)	12.46	12.25
	1.103	364–462		14.81	15.02
	2.999	462–900	Residue of the ligand	41.80	50.56
$CaL_2 \cdot H_2O$	0.228	115–175	$1H_2O$	4.11	3.85
7.001	3.197	175–370	2(CH–O–)	45.66	45.74
Air–Pt	2.002	370–700	2(CH=CH), 3CO with formation of carbonate	28.06	29.05
	0.649	700–740	$1CO_2$	9.27	9.39
7.178	0.284	116–176	$1H_2O$	3.96	3.85
Air–Al_2O_3	3.278	176–400	2(CH–O–)	45.67	45.74
	2.073	400–700	2(CH=CH), 3CO with formation of carbonate	28.87	29.05
	0.650	700–756	$1CO_2$	9.06	9.39
7.108	0.265	130–200	$1H_2O$	3.84	3.85
CO_2–Pt	3.232	200–540	2(CH–O–)	45.47	45.74
	2.061	540–820	Residue of ligand with formation of carbonate	29.00	29.05

Table 2 *(Continued)*

Compound m_i/mg condition	Mass loss/ (mg)	Temp. range/°C	Attribution	Mass loss%	
				Obs.	Calcd.
7.135	0.271	130–206	$1H_2O$	3.80	3.85
CO_2–Al_2O_3	3.257	206–600	2(CH–O–)	45.64	45.74
	2.082	600–876	Residue of ligand with formation of carbonate	29.18 29.18	29.05 29.05
$SrL_2 \cdot H_2O$	0.245	70–120	$1H_2O$	3.47	3.49
7.052	2.927	204–440	2(CH–O–)	41.51	41.52
Air–Pt	1.864	440–575	Residue of ligand with formation of carbonate	26.43	26.38
7.135	0.250	80–130	$1H_2O$	3.50	3.49
Air–Al_2O_3	2.973	210–474	2(CH–O–)	41.67	41.52
	1.882	474–600	Residue of ligand with formation of carbonate	26.37	26.38
7.140	0.245	95–140	$1H_2O$	3.43	3.49
CO_2–Pt	2.965	250–520	2(CH–O–)	41.53	41.52
	1.872	520–750	Residue of ligand with formation of carbonate	26.22	26.38
7.075	0.244	104–158	$1H_2O$	3.45	3.49
CO_2–Al_2O_3	2.937	250–566	2(CH–O–)	41.51	41.52
	1.861	566–900	Residue of ligand with formation of carbonate	26.30	26.38
BaL_2	3.433	240–500	2(CH–O– –CH–CH)	48.56	48.63
7.070	0.623	500–900	Residue of ligand with formation of carbonate and carbonaceous residue	8.81	15.34
Air–Pt					
7.076	2.760	240–440	2(CH–O–)	39.01	39.12
Air–Al_2O_3	1.031	440–610	2(CH=CH), 1CO	14.57	14.62
	0.704	610–900	Residue of ligand with formation of carbonate and carbonaceous residue	9.95	10.23
7.136	3.129	280–544	2(CH–O–)	43.85	43.87
CO_2–Pt	1.351	544–900	Residue of ligand with formation of carbonate and carbonaceous residue	18.94	20.10
6.991	2.738	280–550	2(CH–O–)	39.16	39.12
CO_2–Al_2O_3	1.249	550–900	Residue of ligand with formation of carbonate and carbonaceous residue	17.87	24.85

For the Mg, Ca, Sr and Ba compounds, the DSC curves in air atmosphere (Fig. 3(a)–(d)) exhibit endothermic peaks at 120 and 160°C (Mg), 170°C (Ca), and 125°C (Sr), attributed to dehydration, in agreement with the mass losses observed in the TG and DTG curves. The exothermic peak at 215°C (Ca) is attributed to a recrystallization process and the exothermic peaks at 230°C (Sr) and 255°C (Ba) are probably due to a crystalline transition that occurs before the thermal decomposition.

The broad exotherms in the ranges 220–465°C and 465–600°C (Mg); 230–430°C and 430–600°C (Ca); 255–430°C, 430–410°C and 410–600°C (Ba) are attributed to the thermal decomposition of the anhydrous compounds, where the oxidation of the organic matter takes place in consecutive steps. These are in agreement with the TG and DTG curves obtained in air atmosphere.

For the CO_2 atmosphere (Figs. 3(e)–(h)), the DSC curves also exhibit endothermic peaks due to dehydration and they are observed at the same temperature in an air

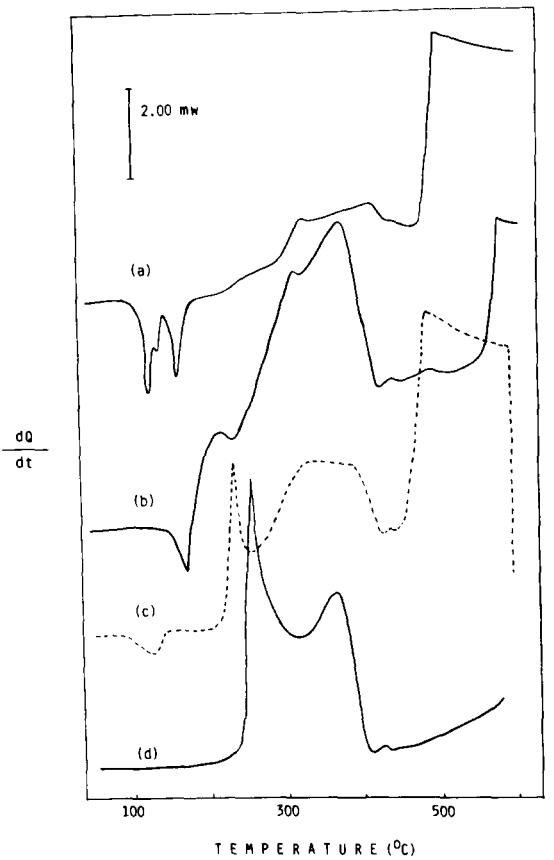

Fig. 3. DSC curves of (a) $Mg(4\text{-}MeO\text{-}BP)_2.4H_2O$ (air); (b) $Ca(4\text{-}MeO\text{-}BP)_2.H_2O$ (air); (c) $Sr(4\text{-}MeO\text{-}BP)_2.H_2O$ (air); (d) $Ba(4\text{-}MeO\text{-}BP)_2$ (air); (e) $Mg(4\text{-}MeO\text{-}BP)_2.4H_2O$ (CO_2); (f) $Ca(4\text{-}MeO\text{-}BP)_2.H_2O$ (CO_2); (g) $Sr(4\text{-}MeO\text{-}BP)_2.H_2O$ (CO_2) and (h) $Ba(4\text{-}MeO\text{-}BP)_2$ (CO_2).

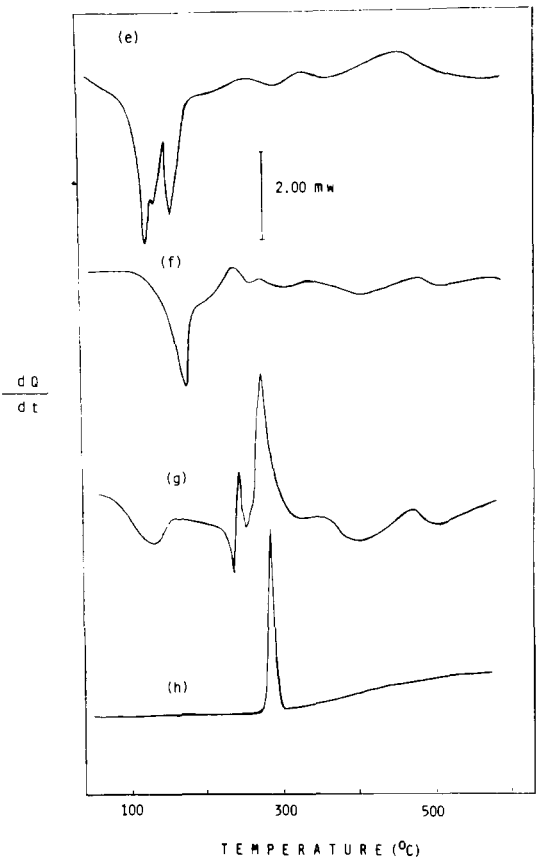

Fig. 3. *(Continued)*

atmosphere. In the calcium compound (Fig. 3(f)), the exothermic peak at 238°C is attributed to a recrystallization process. The sequence of peaks at 236°C (endothermic), 246°C and 277°C (exothermic) in the strontium compound (Fig. 3(g)), and the exothermic peak at 286°C for the barium compound (Fig. 3(h)) are attributed to crystalline transitions.

The sequence of the broad endotherm peaks between 200 and 600°C (Mg), 250 and 600°C (Ca) and 310 and 600°C (Sr), is due to the thermal decompositions of the anhydrous compounds which take place in consecutive steps. For the barium compound, these endotherm peaks are not observed. The observed heat in these steps is probably not enough to produce the decomposition of the anhydrous barium compound.

4. Concluding remarks

The X-Ray powder patterns verified that the alkali earth metal compounds studied in this work have a crystalline structure.

The TG, DTG and DSC curves established the stoichiometry of the compounds in the solid state and provided information about the thermal stabilities of the compounds and of the decomposition products. These curves also show that the thermal stability and the mechanism of thermal decomposition of the solid compounds depend on the identity of the metal ion present, as can be seen from the data of this work and from the data of Ref. [4].

Acknowledgements

The authors acknowlege the FAPESP (Proc. 90/2932-4 and 92/2227-4) for financial support.

References

[1] C.B. Melios, M. Molina and F. Martins, Cienc. Cult. (São Paulo) (Suppl.), 27(7) (1975) 109.
[2] C.B. Melios, J.T. Souza Campos, M.A.C. Mazzeu, L.L. Campos, M. Molina and J.O. Tognolli, Inorg. Chim. Acta, 139 (1987) 163.
[3] C.B. Melios, M. Ionashiro, H. Redigolo, M.H. Miyano and M. Molina, Eur. J. Solid State Inorg. Chem., 28 (1991) 291.
[4] L.C.S.de Oliveria, C.B. Melios, M. Spirandeli Crespi, C.A. Ribeiro and M. Ionashiro, Thermochim. Acta, 219 (1993) 215.
[5] M. Raimer, J. Am. Chem. Soc., 48 (1926) 2459.
[6] H.A. Flaschka, EDTA Titrations, 2nd edn., Pergamon Press, New York, 1964, p. 159, 179, 230, 242, 245, 252, 260, 295.